Pinning Susceptibility: The Effect of Dilute, Quenched Disorder on Jamming

Amy L. Graves, Samer Nashed, Elliot Padgett, Carl P. Goodrich, Andrea J. Liu, and James P. Sethna

Phys. Rev. Lett. **116**, 235501 — Published 10 June 2016

DOI: 10.1103/PhysRevLett.116.235501

Pinning Susceptibility: The effect of dilute, quenched disorder on jamming

Amy L. Graves (formerly, Bug)[1], Samer Nashed[1], Elliot Padgett[1,2],
Carl P. Goodrich[3], Andrea J. Liu[3] and James P. Sethna[4]
[1] *Dept. of Physics and Astronomy, Swarthmore College,*
[2] *School of Applied and Engineering Physics, Cornell University,* [3] *Dept. of Physics and Astronomy, University of Pennsylvania,* [4] *Department of Physics, Cornell University*
(Dated: May 16, 2016)

We study the effect of dilute pinning on the jamming transition. Pinning reduces the average contact number needed to jam unpinned particles and shifts the jamming threshold to lower densities, leading to a pinning susceptibility, χ_p. Our main results are that this susceptibility obeys scaling form and diverges in the thermodynamic limit as $\chi_p \propto |\phi - \phi_c^\infty|^{-\gamma_p}$ where ϕ_c^∞ is the jamming threshold in the absence of pins. Finite-size scaling arguments yield these values with associated statistical (systematic) errors $\gamma_p = 1.018 \pm 0.026(0.291)$ in $d = 2$ and $\gamma_p = 1.534 \pm 0.120(0.822)$ in $d = 3$. Logarithmic corrections raise the exponent in $d = 2$ to close to the $d = 3$ value, although the systematic errors are very large.

In jammed packings of ideal spheres, particles are locked into position by their repulsive interactions with their neighbors, which in turn are locked into position by their neighbors, and so on, so that the entire system is mechanically stable. Pinning is an alternate way of locking a particle into place, so the interplay of pinning and jamming can potentially lead to interesting new behavior. Pinning is known to have a rich interplay with glassiness; pinning raises the glass transition [1] and can be used to probe its nature [2, 3] and associated length scales [3, 4]. In jammed systems, pinning lowers the jamming density [5, 6] and allows access to length scales [7]. Here we show that the addition of quenched disorder in the form of random pinning has a singular effect on jamming. In the dilute pinning limit, jamming is highly susceptible to pinning, with a "pinning susceptibility" that diverges at the jamming transition as a power law in the thermodynamic limit.

In spin systems such as the Ising model, the magnetic susceptibility can be calculated by considering the response to "ghost spins" or especially-designated spins [8] in the limit that their density vanishes; similarly, in percolation or correlated percolation one can calculate susceptibilities to "ghost" sites or bonds [9, 10] that are vanishingly probable. Here, we consider the response to "ghost pins." Systems of N particles, of which a fraction n_f are pinned, are prepared by quenching infinitely rapidly from infinite temperature, $T = \infty$, to $T = 0$ at a volume fraction ϕ. We calculate the fraction of such systems that are jammed, or equivalently, the probability that a state prepared in such a way is jammed, $p_j(\phi, N, n_f)$. We then define the pinning susceptibility in the limit of vanishing pinning:

$$\chi_p = \lim_{n_f \to 0} \frac{\partial p_j(\phi, N, n_f)}{\partial n_f} \tag{1}$$

We find that $\chi_p(\phi, N)$ and the probability of being jammed, $p_j(\phi, N, n_f)$ obey scaling form and that χ_p diverges in the infinite size limit.

There have been two distinct approaches to studying scaling near the jamming transition: in terms of a configuration-dependent or infinite-system critical point. Each finite jammed configuration of particles, Λ, has its own critical volume fraction ϕ_c^Λ, which converges to a single value ϕ_c^∞ only for infinite system sizes [11–13]. For many purposes, scaling behavior near jamming is best done by measuring the deviation from the configuration-dependent critical density (as suggested by Refs. [11, 14]). Here, since we are studying the convergence of the distribution of the configuration-dependent critical densities to the infinite-system critical density, we naturally make use of the other approach, scaling in terms of deviation from ϕ_c^∞. The existence of two distinct scaling pictures is seen in many other systems with sharp, global transitions in behavior, as originally discovered in the depinning of charge-density waves [15–17]. Such systems may not obey the inequality between the correlation length and dimension $\nu \geq 2/d$ derived for equilibrium systems, unless analyzed using deviations from the infinite-system critical point [18, 19].

To study the pinning susceptibility, we conducted numerical simulations on packings of N repulsive soft spheres in d dimensions [11, 14] at fixed area (two dimensions, $d = 2$) or volume ($d = 3$) in a square ($d = 2$) or cubic ($d = 3$) box with periodic boundary conditions. We considered 50:50 mixtures of disks ($d = 2$) or spheres ($d = 3$) with a diameter ratio of 1.0:1.4. Particles i and j with radii R_i and R_j interact with pairwise repulsions

$$U(r_{ij}) = \frac{\varepsilon}{\alpha}\left(1 - \frac{r_{ij}}{R_i + R_j}\right)^\alpha \Theta\left(1 - \frac{r_{ij}}{R_i + R_j}\right) \tag{2}$$

with $\alpha = 2$ (harmonic) or $\frac{5}{2}$ (Hertzian) .

The initial position of each particle was generated randomly, and the positions of $N_f = n_f N$ particles (chosen at random) were fixed. Configurations in which fixed particles overlap were excluded. We then minimized the energy of the system to obtain jammed packings. The upper inset of Fig. 2 contains a sample configuration for $N = 256, N_f = 2$.

We calculated the jamming probability $p_j(\phi, N, n_f)$ at $T = 0$ for systems of size $N = 600, 1000, 2000$ and 4000

in $d = 2$, and $N = 800, 1600, 2400$ and 3200 in $d = 3$. For the small fractions of fixed particles studied here, the criterion for judging a system to be jammed is the same as in previous studies [20]: jammed systems have positive bulk moduli, energies and pressures.

As for systems with no pinned particles, we find that systems with dilute random pinning are isostatic at the onset of jamming. In agreement with earlier studies on jammed hard sphere systems with dilute pinning [6], we find that dilute pinning can result in a generalized isostatic condition. One must distinguish between two types of contacts: the number N_{mm} between two particles which are mobile during equilibration, and the number, N_{mf}, between one mobile and one fixed particle. Each of the N_f fixed particles requires no contacts to be stable, while each of the $N_m = N - N_f$ mobile particles require, on average, a minimum of Z_{iso} contacts. When $N_f = 0$, $N_m = N$ and $Z_{iso} = 2d - \frac{2d}{N_m} + \frac{2}{N_m}$, where the second term arises from d zero modes associated with global translations allowed by translational invariance, and the third term is needed to ensure a nonzero bulk modulus [20]. Our equilibration protocol breaks translational invariance when $N_f \geq 1$; thus in this case $Z_{iso} = 2d + \frac{2}{N_m}$. Since the average number of contacts for a mobile particle is $Z_m = (2N_{mm} + N_{mf})/N_m$, the number of excess contacts that constrain mobile particles is $N_{excess} = N_m(Z_m - Z_{iso})$, or

$$N_{excess} = N_{mm} + N_{mf} - dN_m + dq - 1 \qquad (3)$$

where $q = 1$ for $N_f = 0$, and $q = 0$ for $N_f > 0$. Fig. 1a shows that this relationship is upheld: isostaticity means that the excess number of contacts approaches zero as $p \to 0$. Additionally, Fig. 1a shows scaling collapse onto universal curves as function of rescaled pressure, $p^{1/2}N$. This is exactly the same as what is observed for systems without pins [20]. Note that Fig. 1a is analogous to Fig. 2c of Ref. [20] in the absence of pins, which shows not only the region of slope 1, but crossover to a slope of 2 at very low pressures, arising from a Taylor expansion of $(Z - Z_{iso})$ in p for finite systems. In Fig. 1a there is perhaps the hint of a crossover to a higher slope at $p^{1/2}N \lesssim 1$, but the data are quite noisy at such low pressures.

One might expect that since pinned particles support mobile ones, the number of mobile contacts will decrease with increasing pin density. Indeed, for all pressures studied, increasing n_f decreases the average number of mobile contacts, Z_m. (The only exception is a slight, but nevertheless reproducible, uptick between $N_f = 0, 1$, related to the loss of translational invariance.) Fig. 1b shows Z_m broken down into Z_{mm} arising from mobile-mobile contacts, $Z_{mm} \equiv 2N_{mm}/N_m$, and Z_{mf} from mobile-fixed contacts. At a pressure low enough to approximate the jamming threshold (circles), the average contact number $Z_m(n_f)$ (filled circles) is well-fit by the dashed line shown. Interestingly, raising the pressure by a couple of orders of magnitude does not result in significant changes in $Z_{mf}(n_f)$ (red symbols). In Fig. 1b,

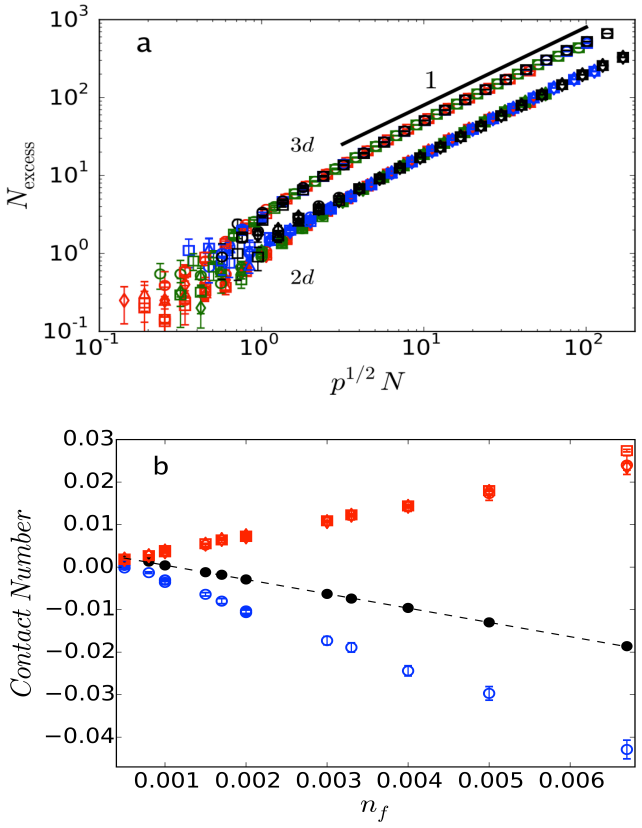

FIG. 1. a: Excess contacts as a function of rescaled pressure. $d = 2$ and $d = 3$ systems are as marked. $N = 600, 1000, 2000, 4000$ colors are red, green, blue, black. $N = 800, 1600, 2400, 3200$ colors are red, green, blue, black. Symbols for $N_f = 1, 2, 3, 4$ are square, circle, triangle, and diamond. b: Contributions to contact number for mobile particles. $Z_{mm} - 4.0$ are shown as blue, Z_{mf} as red. Symbols for $log_{10}\ p = -6, -5, -4$ are circles, triangles, squares. Filled black circles fit by dashed line are $Z_m - 4.0$ for $log_{10}\ p = -6$.

$Z_{mm} - 4.0$ is contrasted with Z_{mf} to show that mobile-mobile contacts disappear more rapidly than mobile-fixed contacts replace them. Thus, jamming in the presence of pinned particles is an unexpectedly "frugal" process, in terms of its use of mobile particles to produce global mechanical stability.

Increasing n_f raises the probability of jamming at any given value of ϕ, in accord with previous work on jamming in the presence of fixed particles [5, 6]. Increasing N steepens the jamming probability, as in the absence of pinning [11]. These features are illustrated in Fig. 2, which shows the jamming probability $p_j(\phi, N, n_f)$ averaged over 10,000-30,000 $d = 2$ systems of size $N = 600$ and 2000, with harmonic repulsions and $N_f = 1, 2, 3$ and 4 fixed particles. The dashed lines in Fig. 2 are fits to a two-parameter logistic sigmoidal form:

$$p_j(\phi, N, n_f) \equiv \frac{1}{(1 + e^{a(-\phi + b)})} \qquad (4)$$

where $a(N, n_f)$ is the "width" of p_j, in that it spans probabilities from $\frac{1}{4}$ to $\frac{3}{4}$; while $b(N, n_f)$ is the value of volume fraction at which $p_j = \frac{1}{2}$. For all N and n_f studied, logistic sigmoid fits to $13 - 21$ independent ϕ values result in χ^2 values less than 0.10. A slightly more flexible three-parameter fit, to "Richard's curve", does not yield significantly better measures of goodness-of-fit.

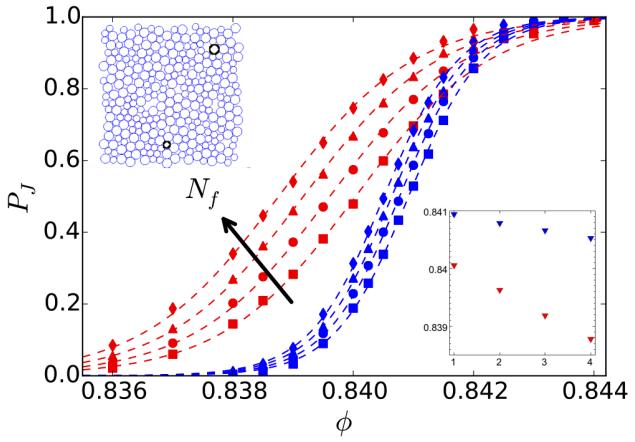

FIG. 2. Probability p_j of jamming as a function of packing fraction, ϕ, in $d = 2$ systems for $N = 600$ (red) and $N = 2000$ (blue). $N_f = 1, 2, 3, 4$ are represented by square, circle, triangle, and diamond symbols, respectively. Dashed curves through data are fits to a logistic sigmoid function. Upper inset: An equilibrated configuration in $d = 2$ with $N_f = 2$. Lower inset: Value of ϕ such that $p_j = 1/2$ for $N = 600$ (red) and 2000 (blue) versus N_f, the number of pinned particles.

We now propose a scaling ansatz for p_j. Since the fraction of pinned sites, n_f, is an independent control parameter with which to approach ϕ_c^∞, a two-variable scaling function can be constructed for the jamming probability. There is significant evidence that the upper critical dimension of the jamming transition is $d_c = 2$ [20–23]. For $d \geq 2$, we therefore expect that finite scaling depends not on linear system size, L, but on particle number N [24]. We therefore propose

$$p_j = F(\Delta\phi\ N^\upsilon, n_f N^{\gamma_p \upsilon}) \tag{5}$$

where $\Delta\phi$ is the distance from the jamming transition for the unpinned, infinite system: $\Delta\phi = \phi - \phi_c^\infty$.

We can rewrite Eq. 4 in terms of the scaling variable $x \equiv \Delta\phi\ N^\upsilon$ as

$$p_j = \frac{1}{(1 + e^{-\tilde{a}xN^{-\upsilon} - \tilde{b}})} \tag{6}$$

with $\tilde{a} = a$ and $\tilde{b} = \phi_c^\infty - ab$. From the logistic sigmoid fits we can obtain functions $\tilde{a}(y)$, $\tilde{b}(y)$, critical exponents γ_p, υ, and the jamming threshold ϕ_c^∞, where $y \equiv n_f N^{\gamma_p \upsilon}$. Because the pinning susceptibility is defined in the dilute pinning limit, we are interested in the limit $n_f \to 0$, or $y \to 0$. (We note that in fitting these quantities to our numerical data on p_j vs. ϕ, the limit $n_f \to 0$ is taken as the limit $N_f \to 1$ and not $N_f \to 0$ since one pin destroys translational invariance. The distinction between $N_f = 0$ and $N_f = 1$ is irrelevant in the limit $N \to \infty$.) We seek the behavior of $\tilde{a}(y)$ and $\tilde{b}(y)$ near $y = 0$:

$$\tilde{a} = a_0 + a_1 y\ ; \quad \tilde{b} = b_0 + b_1 y \tag{7}$$

with higher-order terms in y neglected. Table I shows the parameters in p_j from nonlinear least square fitting in $d = 2$ (four system sizes, four pinning densities) and $d = 3$ (four system sizes, two pinning densities).

	$d = 2$ value	error^a	error^b	$d = 3$ value	error^a	error^b
υ	0.491	0.004	0.045	0.439	0.007	0.051
γ_p	1.018	0.026	0.291	1.534	0.120	0.822
ϕ_c^∞	0.8419	<0.0001	0.0001	0.6472	0.0001	0.0004
a_0	38.555	1.088	12.329	46.177	2.558	17.521
b_0	1.648	0.017	0.193	3.370	0.065	0.442
b_1	9.646	0.879	9.958	2.970	1.145	7.844

TABLE I. Best fit parameters for Eqs. 6, 7. ^{a}Traditional statistical errors. ^{b}Bounds roughly incorporating systematic errors. Estimated from deviations between model and data [25], systematic variance is approximated as twice the best-fit χ^2 divided by the number of parameters.

The parameter a_1 is sufficiently close to zero that it is not listed in Table I. The widths of the sigmoids do not vary significantly with N_f; the principal result of increasing N_f is move the sigmoid to the left, leading to jamming at lower values of ϕ (as in lower inset of Fig. 2).

The scaling ansatz for the jamming probability, Eq. 5, suggests a one-variable scaling ansatz for the pinning susceptibility,

$$\chi_p(\Delta\phi, N) = |\Delta\phi|^{-\gamma_p}\ g_d(\Delta\phi N^\upsilon). \tag{8}$$

Note that we have an explicit form for the function g_d, where $d \geq 2$ is the dimensionality, via Eqs. 1, 6 and 7:

$$g_d(x) = \frac{b_1 e^{b_0 + a_0\ x}}{(1 + e^{bo + ao\ x})^2} \tag{9}$$

We also calculate χ_p for each value of d and N using a finite-difference version of Eq. 1: $\chi_p \approx N \frac{p_j(N_f') - p_j(N_f)}{N_f' - N_f}$ for limitingly small values of N_f', N_f. Using $N_f' = 2$, $N_f = 1$ in the finite difference yields smooth curves for $N = 600, 1000, 2000$ and 4000 in $d = 2$ in Fig. 3a, and for $N = 800, 1600, 2400$ and 3200 in $d = 3$ in Fig. 3b. We have additionally calculated χ_p using pairs of N_f values other than $\{2, 1\}$ (not shown). We find that the finite-difference approximation to χ_p develops a progressively higher peak as $N_f' \to N_f$. Uncertainty in $\chi_p(\phi)$ arises from error in the parameter a (error in b contributes much less) which is fit independently for $p_j(\phi, 2)$

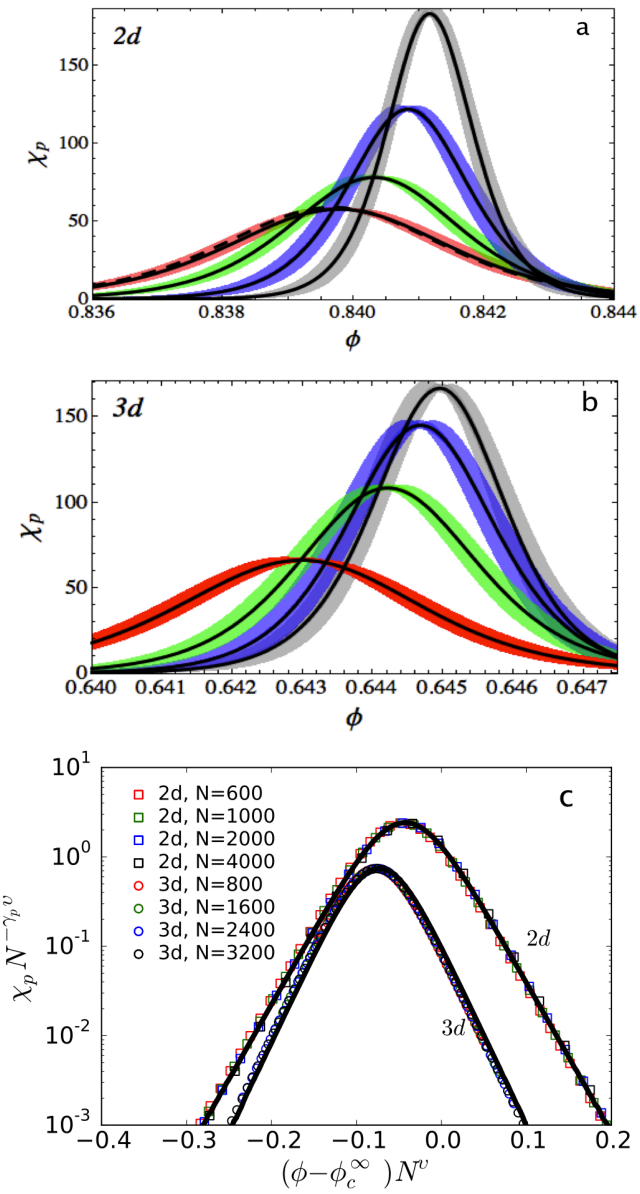

FIG. 3. a: Susceptibility calculated as finite difference for $d = 2$. $N = 600, 1000, 2000, 2000$ with errors as areas around curves in red, green, blue, grey. For $N = 600$, solid line harmonic repulsion and dashed line Hertzian repulsion; all other values of N show harmonic repulsion. b: Susceptibility calculated as finite difference for $d = 3$. $N = 800, 1600, 2400, 3200$ in red, green, blue, grey. c: Universal scaling function (curves, Eq. 9) and finite-difference approximation (points) for non-singular part of pinning susceptibility, $g_d(x)$, for $d = 2, 3$.

and $p_j(\phi, 1)$ before the difference is calculated. This uncertainty is shown as an "envelope" about each curve in Figs. 3a,b. Note that Fig. 3a contains data for both harmonic (solid line) and Hertzian (dashed) potentials for $N = 600$. The disagreement between the two curves is significantly smaller than the error for either curve, supporting the expectation that the pinning susceptibility near criticality is independent of the details of the repulsive potential.

Eqs. 8 and 9 arise from differentiating the scaling form for p_j in Eq. 5 with respect to its second argument. In Fig. 3c, we show the universal functions g_d as curves for $d = 2, 3$. Finite-difference results for different N are shown as points for selected values of $\Delta\phi N^\upsilon$. There is excellent agreement between the points and the curves, indicating that the data at each N are in good agreement with the fitted parameter values in Table I obtained by fitting to data at all N and N_f. The universal function g_d peaks at $x = -0.043$, -0.078 for $d = 2, 3$, respectively. The scaling form of Eq. 8 implies that in the thermodynamic limit, we obtain a power-law divergence of $\chi_p \sim |\Delta\phi|^{-\gamma_p}$.

Note from Table I that the values of ϕ_c^∞ are in excellent agreement with previous work on bidisperse soft spheres [13, 14]. The finite-size exponent υ for $d = 2$ and $d = 3$ is consistent within uncertainty, as expected for systems at or above the upper critical dimension. It is also consistent with the central-limit-theorem value of $\upsilon = 1/2$, identified earlier in the absence of pinning in Ref. [11], and with $\upsilon = 0.465 \pm 0.01$ obtained for $d = 2$ systems by Vågberg, et al. [13], who included power-law corrections to scaling in their analysis.

The pinning susceptibility exponent γ_p in $d = 2$ and $d = 3$ is significantly different when we consider only statistical errors – in contrast to the dimension-independent values expected above the upper critical dimension of two. However, these do not include systematic errors due, say, to choice of theoretical analyses. For example, one way of including logarithmic corrections in $d = 2$, the expected upper critical dimension, leads to a considerably higher value of $\gamma_p = 1.50 \pm 0.95$ (statistical errors). This agrees well with $\gamma_p \sim 1.53$ in $d = 3$, but one must recognize that the estimated range of systematic errors is enormous. As a proxy for exploring different theoretical models, Ref. [25] proposed a method which explores the range of fits that is comparable in residual to the best fit. Following their prescription, we find much larger systematic uncertainties in our estimates of γ_p (Table I). Therefore, our numerical results cannot resolve whether γ_p is the same in $d = 2, 3$.

Indeed, one can argue that γ_p may depend on d as well as a d-independent exponent, ν. Conceptually, the narrowing of the jamming transition with increasing system size [11] and the shift in the average transition [5, 6], imply a derivative of the jamming probability which depends singularly on the density of frozen particles. For attractive pins in $d = 2$ [5], it was noted that average distance between pins, l_f could be equated with a correlation length $\xi \propto \Delta\phi^{-\nu}$ at the jamming threshold. Since $l_f \propto n_f^{-1/d}$, this argument suggests $\Delta\phi \propto n_f^{1/d\nu}$ as a scaling relation. Our Eq. 5 would thus be written $p_j = F(\Delta\phi\ N^\upsilon, n_f N^{\upsilon d\nu})$, implying $\gamma_p \equiv d\nu$. With $\nu = 1/2$ in $d = 2, 3$, this d-dependent prediction for γ_p is consistent with numerical results of Table I.

In summary, we have found that jamming is infinitely susceptible to pinning at the jamming transition in the thermodynamic limit. We have identified a new exponent associated with power-law divergence of this pinning susceptibility. The divergent response to pinning, even in the limit of infinitely dilute pinning, suggests that it should be fruitful to study the interplay of jamming and pinning at higher pinning fractions.

We thank A. A. Middleton for the scaling argument leading to $\gamma_p = d\nu$, and thank R. Kenna for instructive discussions. Acknowledgement is made to the donors of the American Chemical Society Petroleum Research Fund for support of this research, and to the Division of Natural Sciences and Provost's Office of Swarthmore College (ALG, SN, EP). This research was also supported by the US Department of Energy, Office of Basic Energy Sciences, Division of Materials Sciences and Engineering under Award DE-FG02-05ER46199 (AJL, CPG), and by the National Science Foundation under award DMR 1312160 (JPS). This work was partially supported by a Simons Investigator award from the Simons Foundation to AJL and by a University of Pennsylvania SAS Dissertation Award to CPG. ALG was the recipient of a Eugene M. Lang Faculty Fellowship from Swarthmore College in support of sabbatical leave.

[1] K. Kim, Europhys. Lett. **61**, 790 (2003).
[2] C. Cammarota and G. Biroli, PNAS **109**, 8850 (2012).
[3] L. Berthier and W. Kob, Phys. Rev. E **85**, 011102 (2012).
[4] S. Karmakar, E. Lerner and I. Procaccia, Physica A **391**, 1001 (2012).
[5] C.J. Olson Reichhardt, E. Groopman, Z. Nussinov and C. Reichhardt, Phys. Rev. E **86**, 061301 (2012).
[6] C. Brito, G. Parisi and F. Zamponi, Soft Matter **9**, 8540 (2013).
[7] M. Mailman and B. Chakraborty, J. Stat. Mech. **2012**, 1201.0812 (2012).
[8] R.B. Griffiths, J. Math. Phys **8**, 484 (1967).
[9] P.J. Reynolds, H.E. Stanley and W. Klein, J. Phys. A: Math. Gen. **10**, L203 (1977).
[10] J.M. Schwarz, A.J. Liu and L.Q. Chayes, Europhys. Lett. **73**, 560 (2006).
[11] C. S. O'Hern, L. E. Silbert, A. J. Liu and S. R. Nagel, Phys. Rev. E **68**, 011306 (2003).
[12] P. Chaudhuri, L. Berthier and S. Sastry, Phys. Rev. Lett. **104**, 165701 (2010).
[13] D. Vagberg, D. Valdez-Balderas, M. A. Moore, P. Olsson, S. Teitel, Phys. Rev. E **83**, 030303 (2011).
[14] C. S. O'Hern, S. A. Langer, A. J. Liu and S. R. Nagel, Phys. Rev. Lett. **88**, 075507 (2002).
[15] C.R. Myers and J.P. Sethna, Phys. Rev. B **47**, 11171 (1993).
[16] C.R. Myers and J.P. Sethna, Phys. Rev. B **47**, 11194 (1993).
[17] A. A. Middleton and D. S. Fisher, Phys. Rev. B **47**, 3530 (1993).
[18] F. Pazmandi, R. T. Scalettar, and G. T. Zimanyi, Phys. Rev. Lett. **79**, 5130 (1997).
[19] J.T. Chayes, L. Chayes, D.S. Fisher and T. Spencer, Phys. Rev. Lett. **57**, 2999 (1986).
[20] C. P. Goodrich, A. J. Liu and S. R. Nagel, Phys. Rev. Lett. **109**, 095704 (2012).
[21] P. Charbonneau, E. I. Corwin, G. Parisi and F. Zamponi, Phys. Rev. Lett. **109**, 205501 (2012).
[22] P. Charbonneau, J. Kurchan, G. Parisi, P. Urbani and F. Zamponi, J. Stat. Mech, P10009 (2014).
[23] P. Charbonneau, E. I. Corwin, G. Parisi and F. Zamponi, Phys. Rev. Lett. **114**, 125504 (2015).
[24] K. Binder, M. Nauenberg, V. Privman, and A. P. Young, Phys. Rev. B **31**, 1498 (1985).
[25] J.J. Mortensen, K. Kaasbjerg, S.L. Frederiksen, J.K. Norskov, J.P. Sethna and K. W. Jacobsen, Phys. Rev. Lett. **95**, 216401 (2005).